SLAC-PUB-2903
April 1982
(A)

BEAM POLARIZATION MEASUREMENTS AT THE SPEAR STORAGE RING*

J. R. Johnson, R. Prepost and D. E. Wiser†
University of Wisconsin
Madison, Wisconsin 53706

J. J. Murray, R. F. Schwitters‡ and C. K. Sinclair
Stanford Linear Accelerator Center
Stanford University, Stanford, California 94305

ABSTRACT

Radiative beam polarization has been measured in the SPEAR storage ring to determine experimentally the strengths of depolarization phenomena. With single beams, the expected linear depolarization resonances and additional nonlinear and satellite resonances were observed. Data are also presented on polarization with colliding beams.

Submitted to Nuclear Instruments and Methods

---

* Work supported in part by the Department of Energy under contracts DE-AC03-76SF00515 (SLAC) and DE-AC02-76ER00881 (Wisconsin).

† Permanent Address: Stanford Linear Accelerator Center, Stanford, California 94305.

‡ Permanent Address: Physics Department, Harvard University, Cambridge, Massachusetts 02138.

I. INTRODUCTION

Results of extensive measurements of beam polarization at the SPEAR positron-electron storage ring are reported here. These measurements were made to test theories of polarization and depolarization in high energy e^+e^- storage rings and to explore the influence of the beam-beam force on spin motion, where theory provides little guidance.

Beam polarization is an important parameter in high energy e^+e^- colliders because it can affect angular distributions and production rates for many processes of interest. Control of beam polarization makes it possible to study effects that would be inaccessible or difficult to measure with unpolarized beams. For example, transversely polarized beams were used to confirm the spin-1/2 behavior expected for quarks. Longitudinally polarized beams should play an important role at higher energies where weak-electromagnetic interference phenomena are expected to become important.

For the measurements presented here, the beams were polarized by the process of radiative beam polarization (synchrotron radiation with spin-flip). This process provides a practical mechanism where stored beams of electrons and positrons can become highly polarized within a relatively short period of time. The theory of radiative beam polarization is well developed [1] and leads to the result that the natural polarization of positrons (electrons) is parallel (anti-parallel) to the guide magnetic field and, in the absence of depolarizing effects, builds up in time according to:

$$P(t) = \frac{8\sqrt{3}}{15}\left(1 - e^{-t/T_{pol}}\right)$$

$$T_{pol}(s) = \frac{98.7\ r^3}{E^5}\left(\frac{R}{r}\right) \qquad (1)$$

where r is the storage ring bending radius in meters, R is the mean radius, and E is the beam energy in GeV.

The above expressions are valid in the approximation that the magnetic guide field is uniform. Guide fields in real storage rings are not strictly uniform, but vary because of the need to provide focussing and control of various instabilities and because of imperfections arising from construction errors and properties of real magnets. These non-uniformities can lead to a variety of depolarizing phenomena that may limit achievable beam polarizations. Under the simplifying (linear) approximation that variations in the magnetic guide field are proportional to the excursion from the ideal equilibrium orbit, standard accelerator theory techniques can be applied to find the spin motion.

For a particle moving on the equilibrium orbit, the spin motion at any given location on the orbit is described as precession about a fixed axis by a constant angular increment on each successive revolution around the storage ring. The precession direction depends, in general, on the properties of the storage ring guide field and may point in different directions at different locations about the orbit. The number of spin rotations per orbital revolution is called the spin tune ν and is a characteristic frequency of the storage ring. In most cases of interest, the precession direction is parallel to the main bending magnetic field and ν is given by the following:

$$\nu = \frac{\gamma(g-2)}{2} \tag{2}$$

where g is the gyromagnetic ratio of the electron and γ is the Lorentz factor. To a good approximation,

$$\nu \simeq \frac{E\ (\text{GeV})}{0.44065}$$

where E is the beam energy in GeV. Special magnet lattices have been proposed so that the precession direction can be made parallel to the beam direction at special interaction regions. Such lattices allow the possibility of performing experiments using longitudinally polarized beams.

Actual particles in real storage rings do not always follow the equilibrium orbit and the polarization of an ensemble of particles may be diminished by two classes of depolarization effects, called resonant and stochastic depolarization. Resonant depolarization occurs when perturbing fields add coherently to change the spin by large, unpredictable amounts. This may occur when the spin precession frequency equals some characteristic frequency of the storage ring. The resonances are expected to satisfy the conditions:

$$\nu = k \pm \ell\nu_x \pm m\nu_y \pm n\nu_s \tag{3}$$

where k, ℓ, m, and n are integers, ν_x and ν_y are horizontal and vertical betatron tunes, and ν_s is the synchrotron tune, respectively.

Stochastic depolarization arises from the quantum fluctuations and damping in electron storage rings. The basic idea is that the process of quantum emission followed by damping of the resulting betatron motion causes the spin of an initially fully polarized particle to precess away from the vertical direction, thus reducing its polarization. It is evident that vertical orbit distortions and vertical beam size, which cause particles to experience horizontal focussing fields, are major sources of stochastic depolarization. Detailed calculations of resonant and stochastic depolarization using the linear approximation have been performed and computer codes exist to model actual storage rings [2]. The goal of this experiment is to check these models. One known deficiency in the models is that they do not account for nonlinearities of the guide field. The most notable of these is the beam-beam effect, for which there is no satisfactory theory.

In the presence of such depolarizing effects, characterized by a depolarizing time constant T_{depol}, the beam polarization grows with time according to:

$$P(t) = \frac{8\sqrt{3}}{15} \frac{1}{1+x} \left(1 - e^{-t(1+x)/T_{pol}}\right) \qquad (4)$$

where $x \equiv T_{pol}/T_{depol}$ is a convenient quantity to compare with theoretical calculations. Thus under the influence of depolarizing effects, the polarization reaches a smaller asymptotic value and approaches this value more rapidly. In the absence of depolarization the depolarizing time is infinite, hence $x = 0$ and eq. (4) reduces to eq. (1).

II. METHOD

A Compton-scattering polarimeter was used to make the polarization measurements presented here. This technique is described in detail elsewhere [3]. This method was chosen because it is capable of making precise measurements of the polarization of a stored beam in a time short compared with the polarization build-up time. Circularly polarized photons from a laser were focussed on a stored positron beam in SPEAR. A detector measured the vertical angular distribution of the backscattered gamma rays. An up-down asymmetry in the vertical distribution results from spin-dependent terms in the Compton cross section if the positron beam is transversely polarized in the vertical direction.

To determine the beam polarization P_e, an up-down asymmetry A is calculated using the numbers of events in chosen regions of the vertical distribution of backscattered photons:

$$A = \frac{U - D}{U + D} \quad , \tag{5}$$

where U is the number of events in a region above the scattering mid-plane and D is the number of events in a symmetrically placed region below the mid-plane. These regions are chosen to maximize the statistical precision of the measurements. To cancel certain possible false asymmetries due to systematic effects, measurements for both left (L) and right (R) circular polarizations of the laser beam are averaged (with opposite sign):

$$\bar{A} = \left(A_L - A_R\right)/2 \quad . \tag{6}$$

The measured asymmetry $\bar{A}$ is related to P_e by

$$\bar{A} = \Pi P_e \quad , \tag{7}$$

where the analyzing power Π is calculated to be between approximately 2.5% and 3% for the conditions of these measurements, depending on the positron beam energy and the choice of regions U and D.

III. RESULTS

A. Asymmetry Measurements

At typical backscattered rates of 10-15 kHz, over 10^6 events were normally accumulated in a two-minute run, yielding asymmetry measurements with a statistical precision on the order of ±0.001 after subtraction of background. Figure 1 and fig. 2 show sample vertical distributions for positron energies of 2.05 and 3.60 GeV, respectively. Each represents an individual run approximately two minutes in length. In each case the upper graph is the sum of the distributions for left and right circularly polarized incident photons, and the lower graph is the difference. Figure 1(b) shows the flat difference spectrum expected for unpolarized positrons, while fig. 2(b) shows the characteristic asymmetric distribution expected for substantial polarization. The corresponding values of $\bar{A}$ as defined in eqs. (5) and (6) are $(-0.087 \pm 0.096)\%$ and $(2.55 \pm 0.14)\%$, respectively.

Figure 3 shows an example of asymmetry measurements as a function of time during a single SPEAR fill with positrons only. Here the elapsed time was defined to start from zero when the storage ring had finished ramping to its final energy of 3.7 GeV. The solid curve is a fit to the expected time dependence of the beam polarization expressed by eq. (4), and yields a time constant consistent with the theoretical expression of eq. (1), assuming no depolarizing effects ($x = 0$).

Similar measurements and fits have been made at other energies where there was expected to be little depolarization. For each energy, the time constant T_{pol} may be obtained from the fit, assuming $x = 0$. Figure 4 shows fitted time constants for polarization build-up at 2.82, 3.26, and 3.70 GeV. The solid line represents the theoretical expression from eq. (1). The agreement is excellent. For such measurements where the time dependence is consistent with $x = 0$, it is generally true that the fitted asymptotic values are also consistent with the calculated analyzing power times the maximum expected beam polarization of $8\sqrt{3}/15 = 0.924$ from eq. (1), within the systematic and statistical uncertainties. However, for the analysis described below the absolute analyzing power is not assumed to be known and values of x are derived mainly from the time dependence.

B. Energy Scans with Single e^+e^- Beams

Since depolarizing effects are expected to exhibit strong energy dependence, with resonances of various widths and strengths, it is of primary interest to measure the beam polarization as a function of machine energy. A large number of asymmetry measurements can be made over the duration of a SPEAR fill while the beam energy is raised in a series of small steps. Each energy value is maintained long enough to allow a good determination of any change in the asymptotic asymmetry. Figure 5 shows asymmetry measurements as a function of time during a portion of such a scan, covering SPEAR e^+ energies from about 3.60 to 3.64 GeV in 2 MeV steps. The measured asymmetry builds from zero at the beginning of the fill, but tends toward a different asymptotic value for each energy.

In general, over the duration of any one fixed-energy segment of such a scan the asymmetry is expected to vary with time t according to

$$A(t) = \frac{A_f}{1+x} + \left[A_i - \frac{A_f}{1+x}\right] \exp\left[-t(1+x)/T_{pol}\right] \quad . \qquad (8)$$

Here A_i is the asymmetry at the beginning of this segment of the scan and A_f represents the asymptotic asymmetry for the case of no depolarization. Fits of this function for A_i, A_f and x have been made to a number of energy scans, with x constrained to be positive and the entire curve required to be piecewise continuous. The value of A_f is required to be the same for all segments (that is, the analyzing power is assumed not to change appreciably over the energy range of the scan), and T_{pol} is calculated for each energy using eq. (1). The results of such a fit are shown as the solid curve in fig. 5.

The corresponding fitted values of x for the full energy scan, of which fig. 5 shows a portion, are plotted in fig. 6. Three depolarizing resonances are clearly seen in this energy range. This information can perhaps be displayed more clearly by plotting instead the quantity 1/1+x, which gives the ratio of the measured asymptotic beam polarization to the maximum asymptotic value of 0.924 corresponding to the case of no depolarization. Figure 7 shows the same data as the previous figure, but replotted in the manner just described. On the horizontal axis are indicated three energy values which satisfy the general condition for resonant depolarization [eq. (3)] with low-order combinations of the characteristic frequencies of orbital motion in the storage ring. The positions of the observed depolarizing resonances in this energy region are in excellent agreement with these values.

The solid line in fig. 7 represents a calculation by Chao [2] for a typical SPEAR configuration. It is characteristic of the matrix method used that the nonlinear resonance $\nu - \nu_x + \nu_s = 3$ is not predicted by the calculation. The other two (linear) resonances are in excellent agreement with the prediction. The width of the observed resonance $\nu - \nu_y = 3$ is greater than that calculated, but is consistent with being dominated by the natural spread in the vertical betatron tune ν_y, as indicated on the figure. The width of the resonance $\nu - \nu_x = 3$ is considerably larger than the appropriate tune spread, and is reasonably well reproduced by the calculation.

Many such energy scans were made during the course of this experiment, and in general the betatron and synchrotron tunes were slightly different from scan to scan. To allow superposition of such data, the energy scale for points in the vicinity of a resonance can be shifted to compensate for known shifts in the appropriate tunes ν_x, ν_y, and ν_s, since the spin tune ν is directly related to the energy by eq. (2). Figure 8 shows a compilation of all the single-beam (e^+ only) data taken for energies greater than 3.5 GeV. (Most of the polarimeter running time was spent in this energy region, since only there is T_{pol} small enough (~15 minutes) to allow many small energy steps to be studied in a reasonable length of time.) The solid line in the figure is hand-drawn to guide the eye. Again the observed depolarizing resonances are identified with low-order combinations of tunes that add up to an integer, as indicated below the horizontal axis. It can be seen that in addition to the dominant integer resonance $\nu = 8$, the first-order betatron sidebands $\nu - \nu_x = 3$ and $\nu - \nu_y = 3$, the nonlinear resonances $(\nu - \nu_x) \pm \nu_y$ = integer and the synchrotron satellite resonances $(\nu - \nu_y) \pm \nu_s$, $(\nu - \nu_x) \pm 2\nu_s = 3$ are all present in the data. The synchrotron sidebands $\nu - \nu_s = 3$ and $\nu - 2\nu_s = 3$ are not indicated due to the low density of data points in the region between 3.52 and 3.56 GeV. Any other possible resonance combinations in this region seem to be too weak to observe.

C. ν_y Scan at Fixed Energy

Given a depolarizing resonance satisfying the general condition expressed by eq. (3), a measurement of the appropriate frequencies of particle motion ν_x, ν_y, and ν_s at the center of the resonance constitutes a measurement of the spin precession frequency ν. Since ν is related to the beam energy E by eq. (2), this measurement provides a precise energy calibration of the storage ring.

In the preceding section, depolarizing resonances were traversed by varying the beam energy. For this measurement the chosen resonance, described by $\nu - \nu_y = 3$, was scanned by keeping E fixed and varying instead the appropriate betatron frequency ν_y. This resonance was chosen for several reasons.

(a) It has been observed to be relatively narrow, thus allowing a precise determination of the central frequency.

(b) It is of first-order, and is therefore comparatively strong and reproducible. Furthermore, when sweeping through the resonance only E and ν_y need be controlled carefully.

(c) Of all resonances satisfying (a) and (b), this particular resonance appears at the highest available SPEAR energy (about 3.6 GeV since ν_y is about 5.2). This minimizes the relative error in ν due to measurement error in the central value of ν_y. The high energy also provides a characteristic polarization build-up time constant short enough (about 15 minutes) to allow a number of finely spaced measurements through the resonance during the lifetime of the stored beam.

During this scan, ν_y was varied from 5.178 to 5.186 in steps of 0.001. For each point, the betatron frequency spectrum was measured and recorded. A typical spectrum is shown in fig. 9, displaying a rather large spread in ν_y, presumably due to power supply ripple. The value of ν_y assigned to each point is the most probable value of the distribution. At each setting, enough up-down asymmetry measurements were made to allow a good determination of the beam polarization through the analysis described earlier. These values are plotted versus ν_y in fig. 10. The vertical error bars represent the statistical errors on the fitted values of $1/1+x = P/0.92$, and the horizontal error bars indicated the spread in ν_y at half-height on the distribution, as shown in fig. 9. A clear resonance dip is evident. Judging these results both from the most probable values of ν_y and from the tune-spread, we estimate conservatively that the central value of the resonance is given by

$$\nu_y = 5.1835 \pm 0.0015 \quad .$$

Hence the spin-precession frequency for this setting of SPEAR is

$$\nu = 3 + \nu_y = 8.1835 \pm 0.0015 \quad .$$

Therefore the absolute energy of SPEAR for those runs was

$$E = (3.6061 \pm 0.0007) \text{ GeV} \quad .$$

Previously, the energy calibration of the storage ring was obtained from magnetic measurements. During these runs, readings were taken from a calibrated flip coil in a standard magnet. Applying the known flip coil calibration factor, taking into account the measured saturation properties of the various SPEAR bending magnets, and correcting for orbit errors, trim fields and the earth's magnetic field, the corresponding beam energy is determined to be

$$E = 3.6052 \text{ GeV}$$

with an estimated systematic uncertainty of ±0.1%. These values agree within the quoted uncertainty.

Alternatively, these results may be interpreted as a measurement of the positron magnetic anomaly $a_{e^+} = (g_{e^+} - 2)/2$ at high energy ($\gamma = 7.06 \times 10^3$). The value obtained is

$$a_{e^+} = 1.1599 \ (12) \times 10^{-3} \quad ,$$

to be compared with the best value for a_{e^+} measured near rest [4]

$$a_{e^+} = 1.159652222 \ (50) \times 10^{-3} \quad .$$

D. Colliding Beam Results

There exists no satisfactory theory to calculate the effect of beam-beam collisions on the beam polarization. Experimentally, near the upper end of the SPEAR energy range (> 3.5 GeV) it is possible to have fairly stable and reproducible polarization conditions with colliding beams. Indeed, the first observation of polarization with colliding beams at SPEAR was made at 3.7 GeV in a high-energy physics experiment [5], and the first asymmetry measurements with this polarimeter were made with the beams colliding at this same energy. The backscattered laser technique was found to work as well with colliding beams as with a single e^+ beam, with no loss in signal/noise ratio or analyzing power.

Figure 11 shows results from an energy scan with colliding beams near the resonance $\nu - \nu_y = 3$. As compared with the corresponding single-beam results already shown, two effects are evident:

(a) The resonance appears at a higher energy, due to the expected linear beam-beam tune shift.

(b) The resonance is also considerably broadened, consistent with the expected increased spread in ν_y.

A substantial amount of polarimeter running was done with colliding beams, both during machine studies and normal operation for high-energy physics. An example is shown in fig. 12, from a single SPEAR fill at 3.35 GeV. After initial rapid build-up of the asymmetry to a value corresponding to $P_e \lesssim 50\%$, a subsequent gradual increase is evident, as the beam currents and resulting beam-beam forces diminish. An effect in the opposite direction has been observed with colliding beams at 3.694 GeV [6], with initial polarization build-up close to P_{max} followed by a steady decline with time. In this case a possible interpretation is that a nearby depolarizing resonance (probably $\nu - \nu_y - 2\nu_s = 3$, see fig. 8) is moving closer to the chosen beam energy as the linear beam-beam tune shift decreases with the e^+e^- currents.

In general, however, these measurements were not consistent from week to week and the changes were not usually correlated with known changes in machine conditions, so it is difficult to draw any precise conclusions about beam-beam effects on polarization other than those mentioned above. Extensive further measurements on other storage rings under carefully controlled machine conditions will be required before a quantitative understanding of beam-beam depolarization can be achieved.

ACKNOWLEDGEMENTS

The authors would like to acknowledge the help and participation of G. E. Fischer, D. B. Gustavson, and T. J. Phillips at various stages of this experiment. R. Eisele, A. Gallagher, and J. Jurow made important contributions in the design and implementation of modifications to the SPEAR storage ring. M. Browne, J. Escalera, K. Jobe, M. Lateur, C. Noyer, and E. Taylor provided technical support for instrumentation and installation of experimental apparatus and beam lines. This work was supported in part by the Department of Energy under contracts DE-AC03-76SF00515 (SLAC) and DE-AC02-76ER00881 (Wisconsin).

REFERENCES

[1] A. A. Sokolov and I. M. Ternov, Sov. Phys.-Dokl. 8 (1964) 1203; J. D. Jackson, Rev. Mod. Phys. 48 (1976) 417.

[2] A. W. Chao, Proceedings of the 1980 International Symposium on High-Energy Physics with Polarized Beams and Polarized Targets, Lausanne, Switzerland, September 1980, edited by C. Joseph and J. Soffer.

[3] D. B. Gustavson et al., Nucl. Instrum. Methods 165 (1979) 177.

[4] P. B. Schwinberg, R. S. Van Dyck, Jr. and H. G. Dehmelt, Phys. Rev. Lett. 47 (1981) 1679.

[5] R. F. Schwitters et al., Phys. Rev. Lett. 35 (1975) 1320; G. Hanson et al., Phys. Rev. Lett. 35 (1975) 1609; J. G. Learned et al., Phys. Rev. Lett. 35 (1975) 1688.

[6] Private communication, Crystal Ball Collaboration. This group operated the polarimeter during their experimental running in May 1981.

FIGURE CAPTIONS

1. (a) Sum of and (b) difference between measured vertical distributions of backscattered gamma rays for right and left circularly polarized photons incident on an unpolarized positron beam at an energy of 2.05 GeV. The experimental asymmetry as defined in eq. (6) is $(-0.087 \pm 0.096)\%$.

2. (a) Sum of and (b) difference between backscattered vertical distributions from right and left circularly polarized photons incident on a polarized positron beam at an energy of 3.60 GeV. The measured asymmetry is $(2.55 \pm 0.14)\%$.

3. Measured asymmetry versus time, with 3.7 GeV positrons only circulating in SPEAR.

4. Polarization time constant T_{pol} versus positron beam energy. The data points are the results of fits to the observed build-up of asymmetry with time at three energies. The solid line is the theoretically expected behavior.

5. Asymmetry measurements versus time, for approximately 2 MeV steps of SPEAR energy in the region of 3.60 to 3.64 GeV. The solid line is a fit to eq. (8).

6. Fitted values of $x \equiv T_{pol}/T_{depol}$, from a SPEAR energy scan which includes the data shown in fig. 5.

7. The data of fig. 6 replotted as $1/1+x = P/P_{max}$, where $P_{max} = 0.924$ is the maximum polarization theoretically expected. The solid line is from a calculation by Chao [2].

8. Compilation of results from all single-beam e^+ energy scans in the region of 3.50 to 3.75 GeV. The solid line is hand-drawn to guide the eye. The arrows below the horizontal axis indicate observed depolarizing resonances.

9. Wave analyzer output signal versus driving frequency, for measuring vertical betatron frequency ν_y.

10. Measurements of the ratio P/P_{max} versus vertical betatron frequency ν_y for a fixed SPEAR energy near 3.6 GeV.

11. Measurements of P/P_{max} versus SPEAR energy with e^+e^- colliding beams in the vicinity of 3.6 GeV.

12. Asymmetry measurements versus time with e^+e^- colliding beams at an energy of 3.35 GeV.

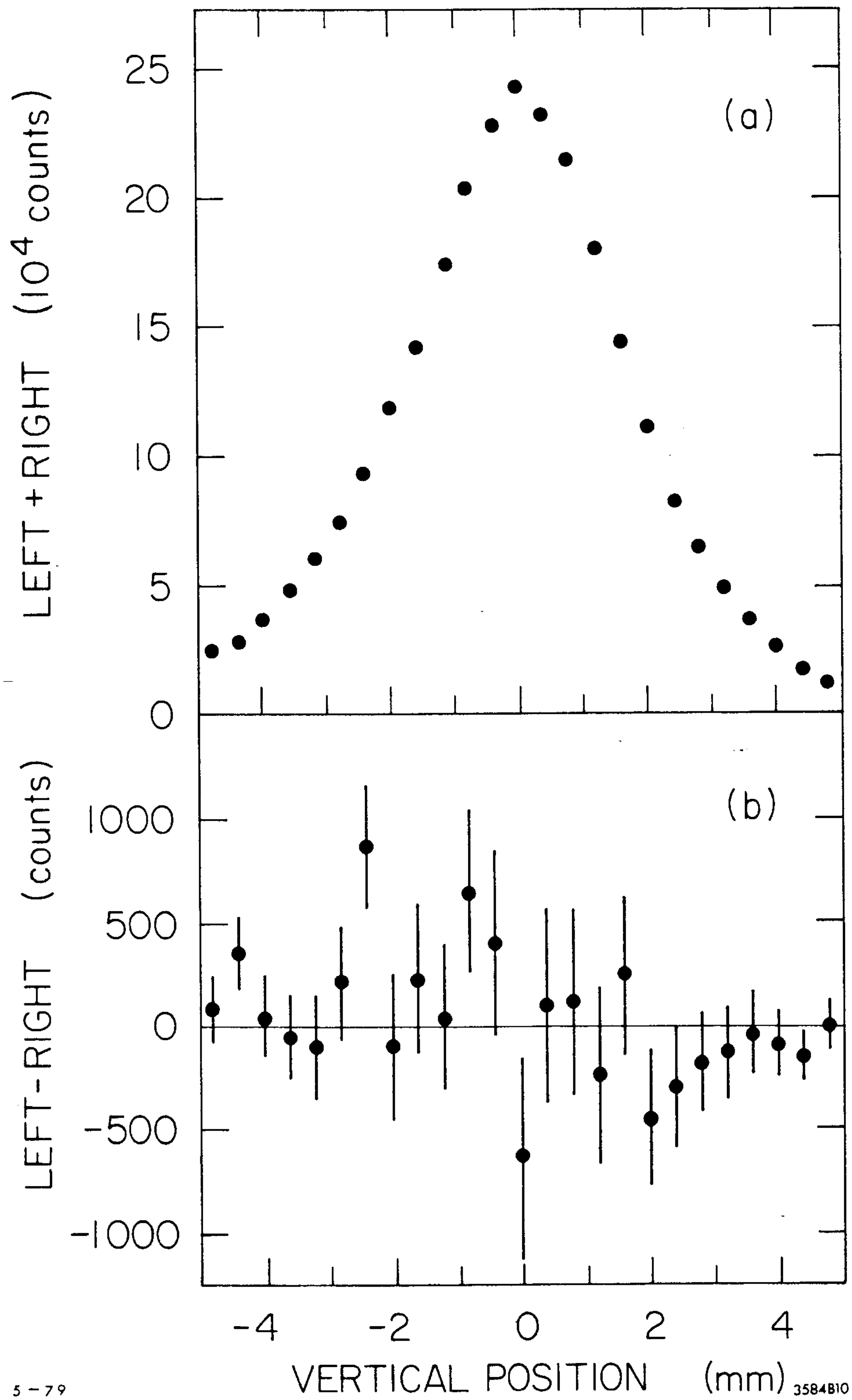

25
20
15
10
5
0
LEFT + RIGHT (10^4 counts)
(a)
1000
500
0
-500
-1000
LEFT - RIGHT (counts)
(b)
-4
-2
0
2
4
VERTICAL POSITION (mm)
5-79
3584B10

Fig. 1

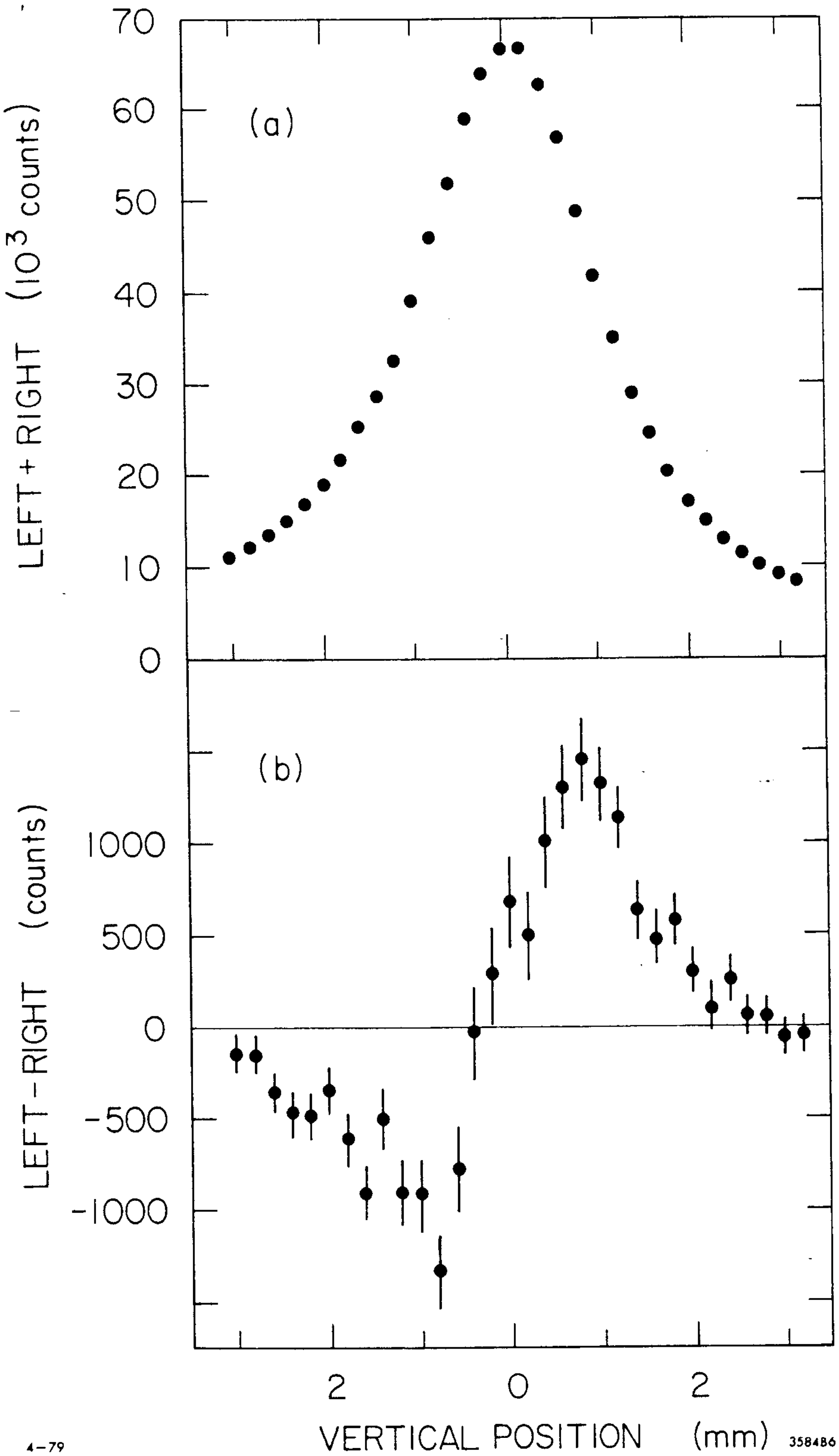

(a)
(b)
LEFT + RIGHT (10^3 counts)
70
60
50
40
30
20
10
0
LEFT - RIGHT (counts)
1000
500
0
-500
-1000
2
0
2
VERTICAL POSITION (mm)
4-79
358486

Fig. 2

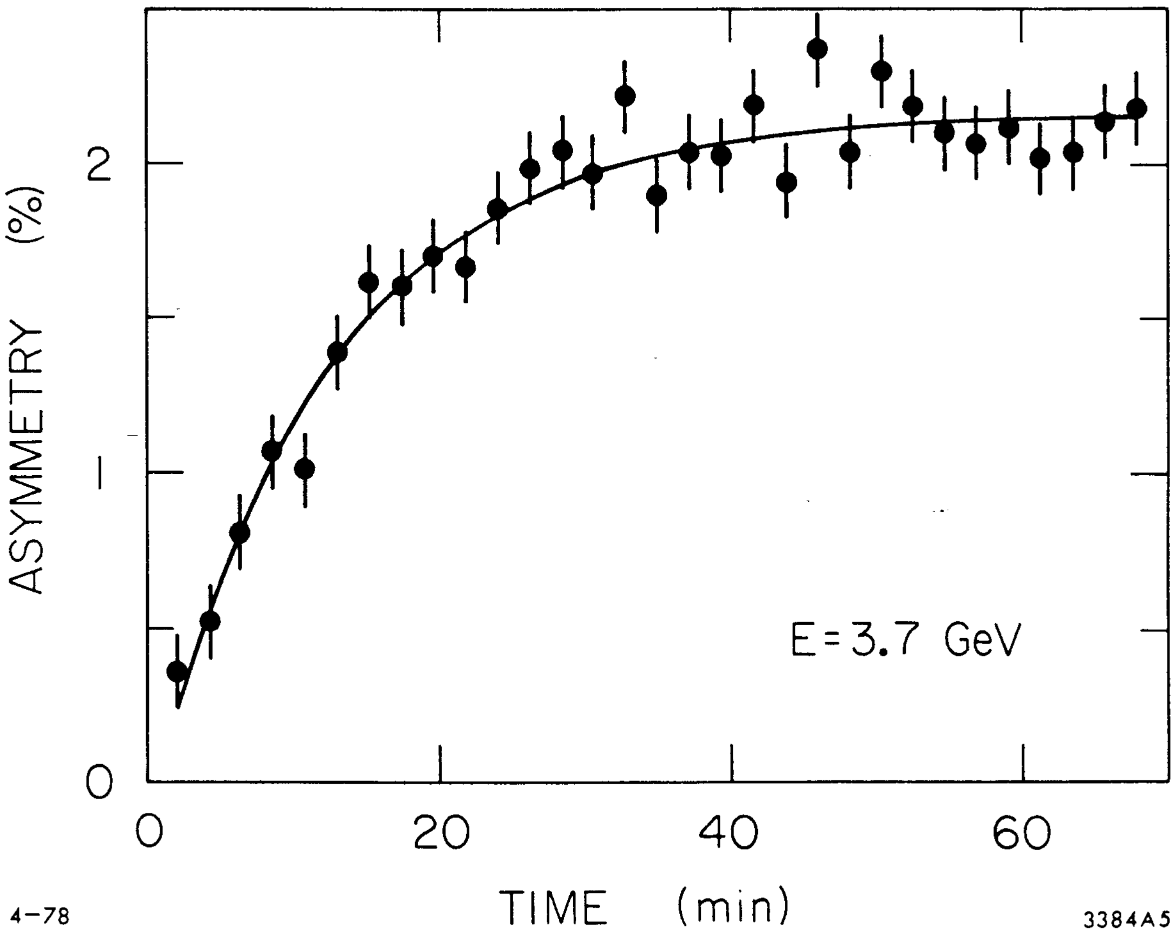

Fig. 3

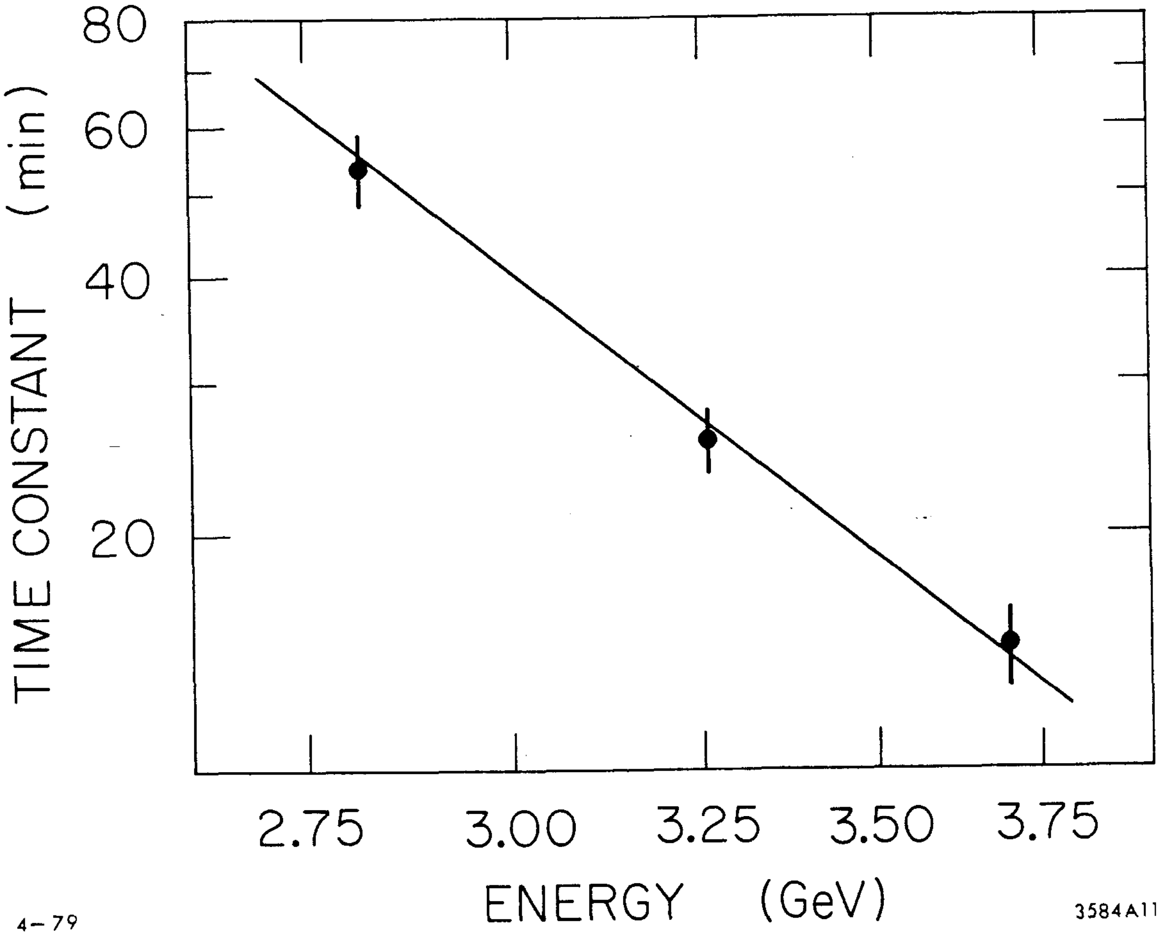
80
60
40
20
TIME CONSTANT (min)
2.75
3.00
3.25
3.50
3.75
ENERGY (GeV)
4-79
3584A11

Fig. 4

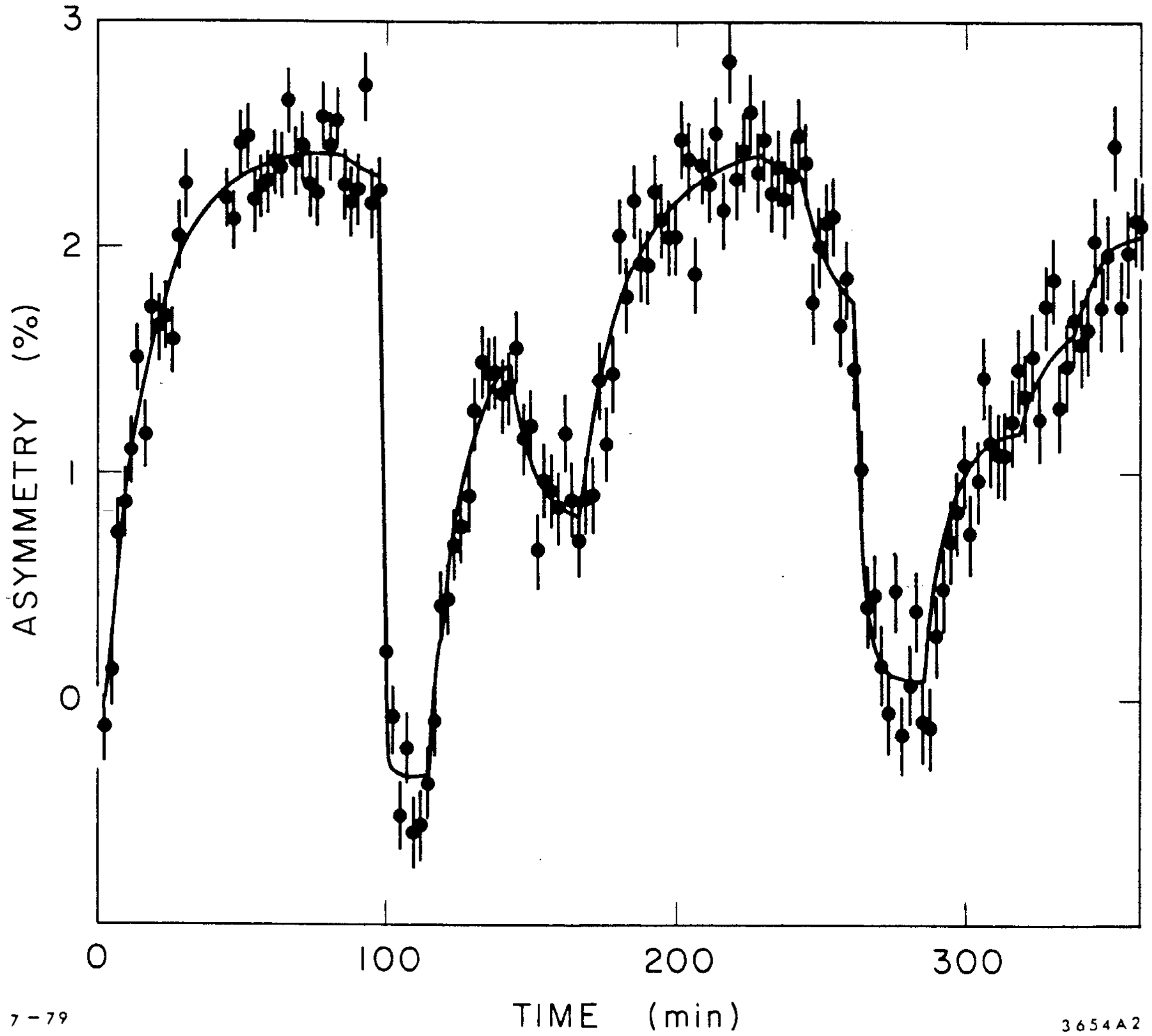

Fig. 5

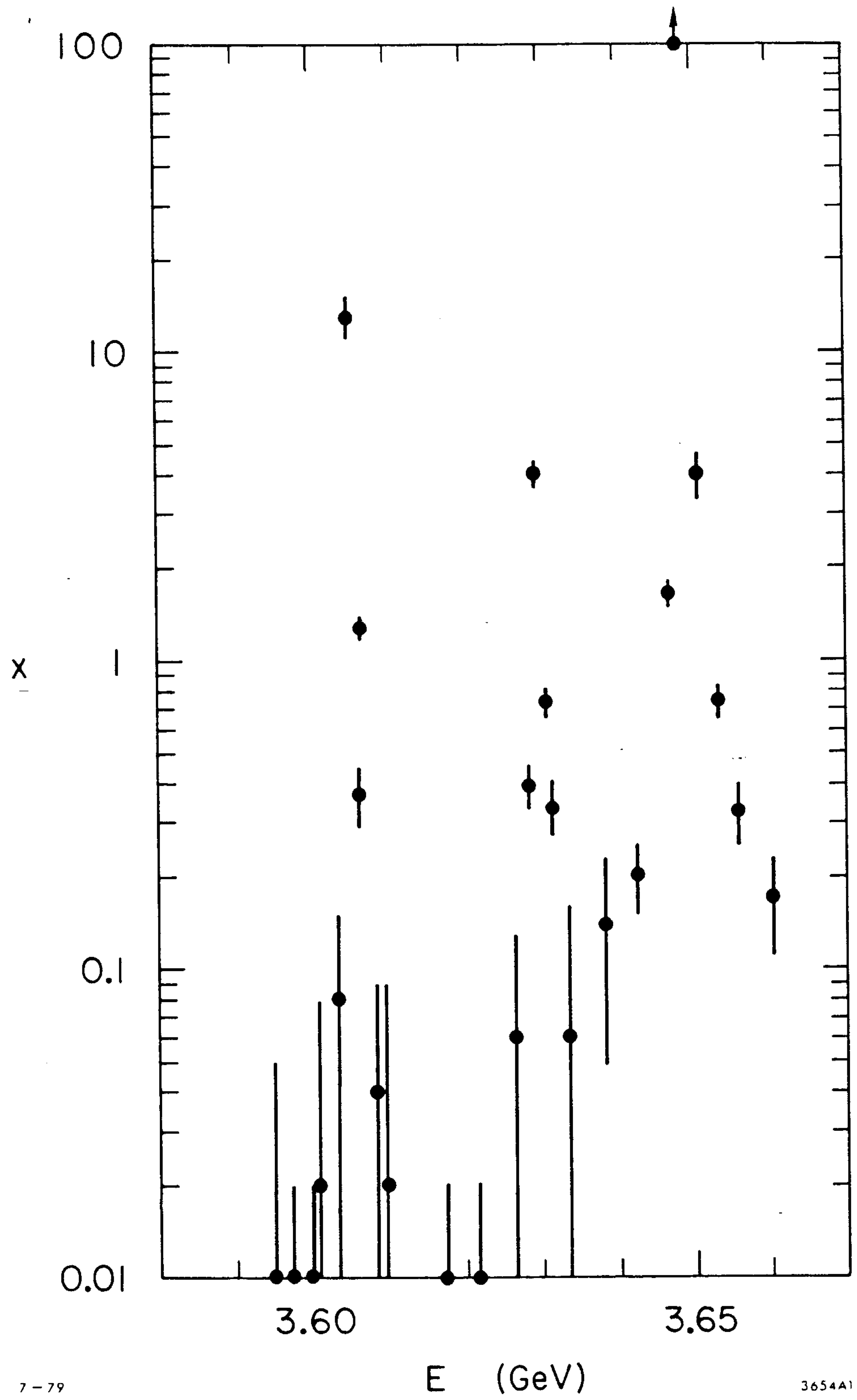

Fig. 6

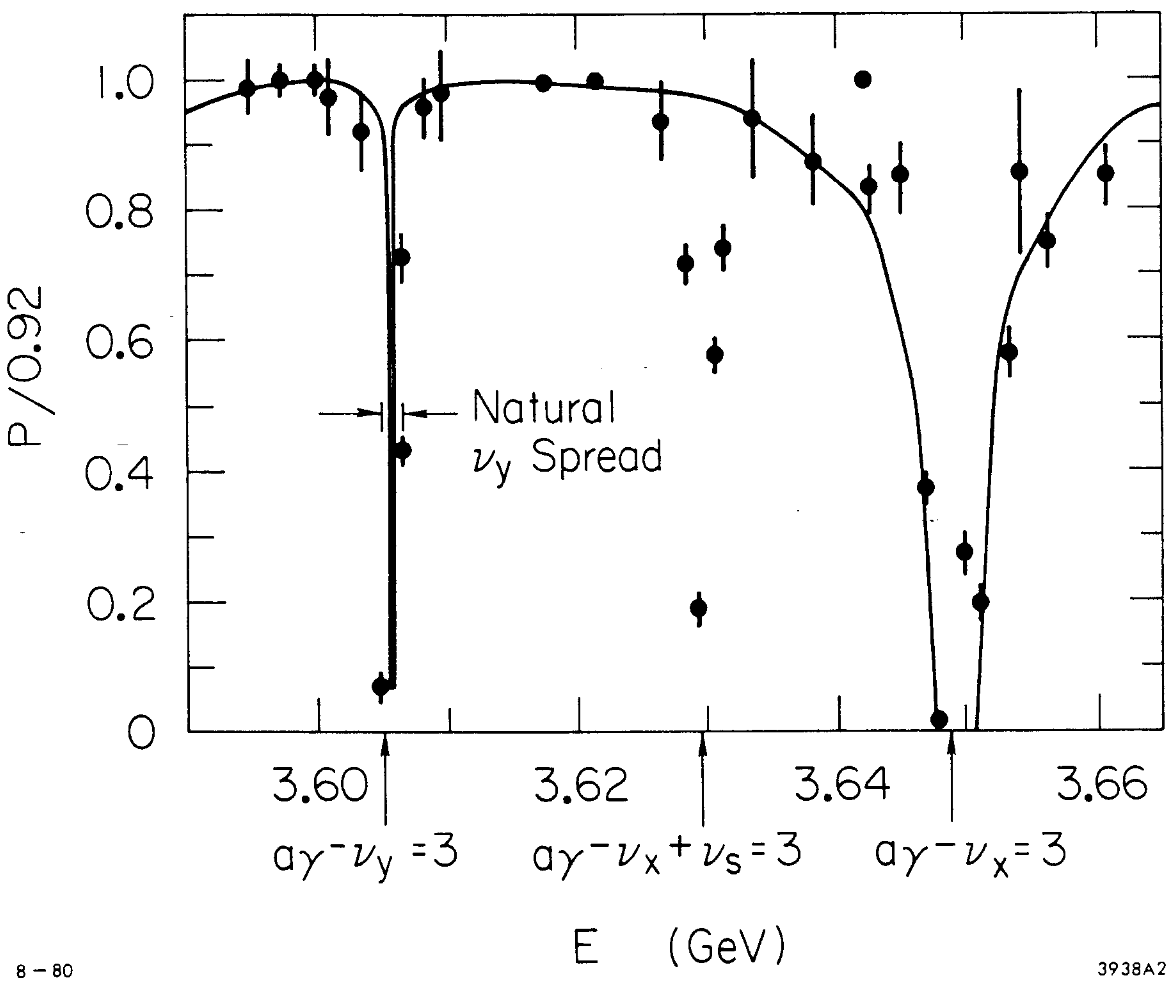

1.0
0.8
0.6
0.4
0.2
0
P/0.92
Natural
ν_y Spread
3.60
3.62
3.64
3.66
$a\gamma - \nu_y = 3$
$a\gamma - \nu_x + \nu_s = 3$
$a\gamma - \nu_x = 3$
E (GeV)
8 – 80
3938A2

Fig. 7

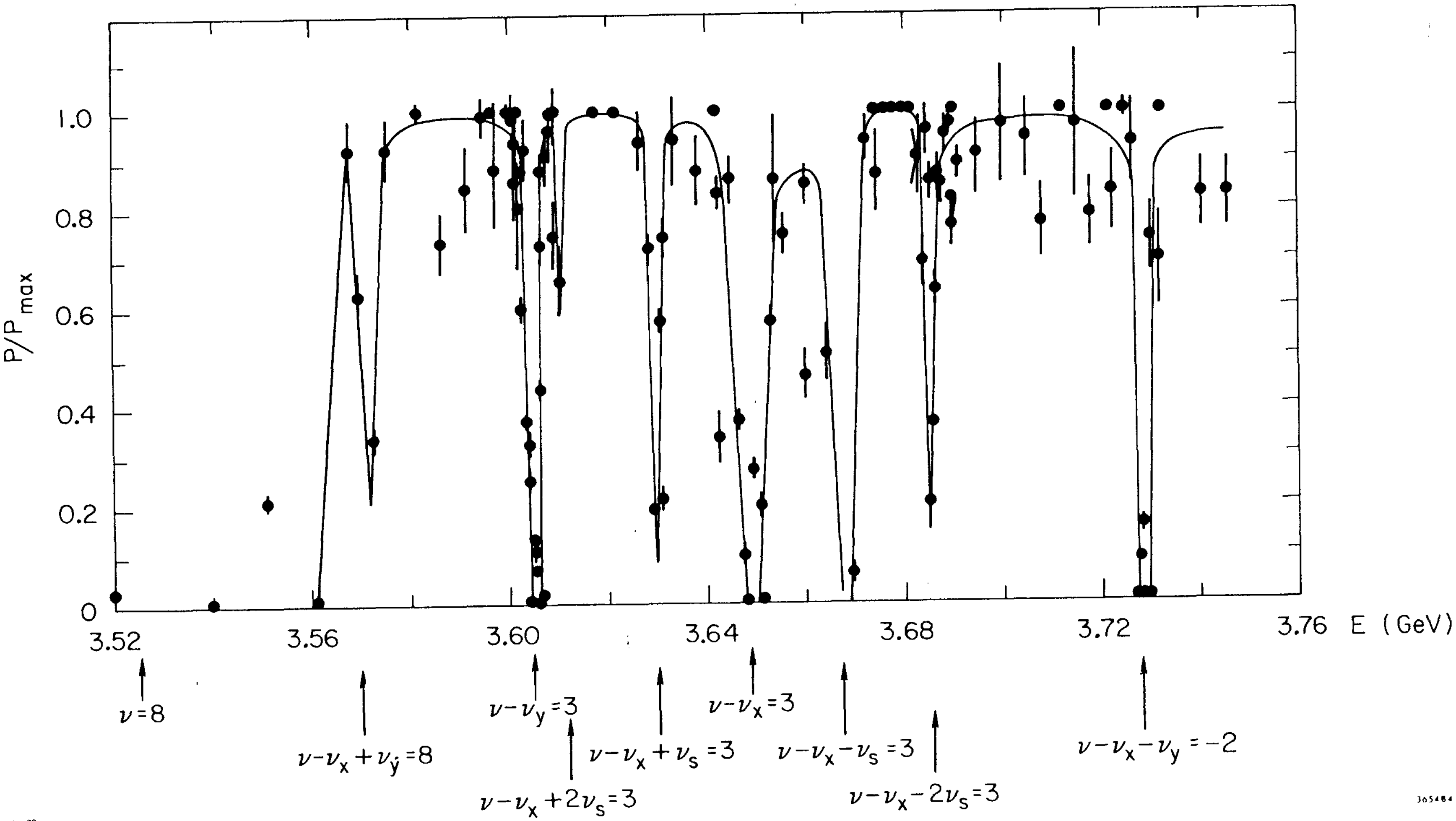

8-79

365484

Fig. 8

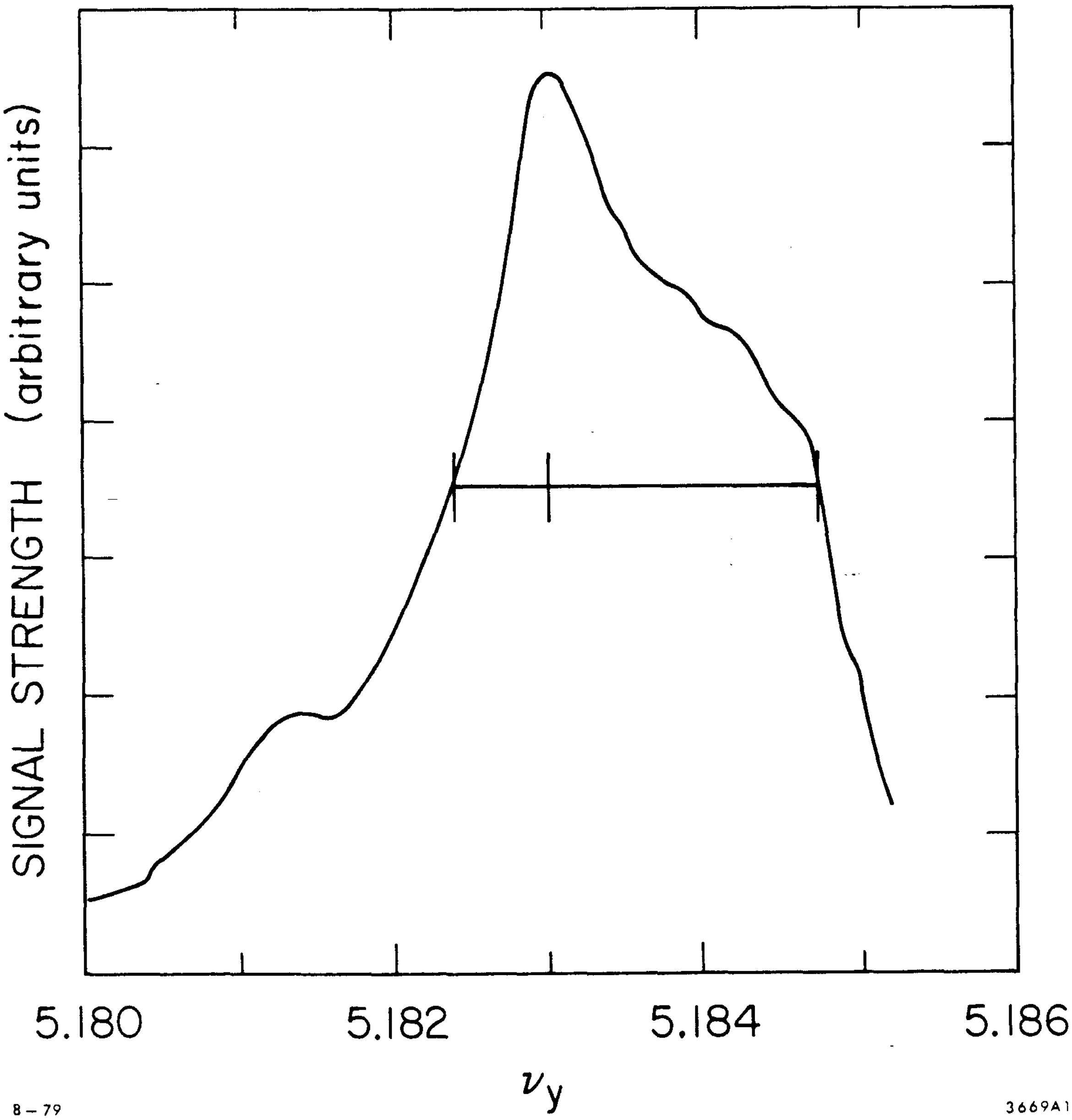
SIGNAL STRENGTH (arbitrary units)
5.180
5.182
5.184
5.186
ν_y
8-79
3669A1

Fig. 9

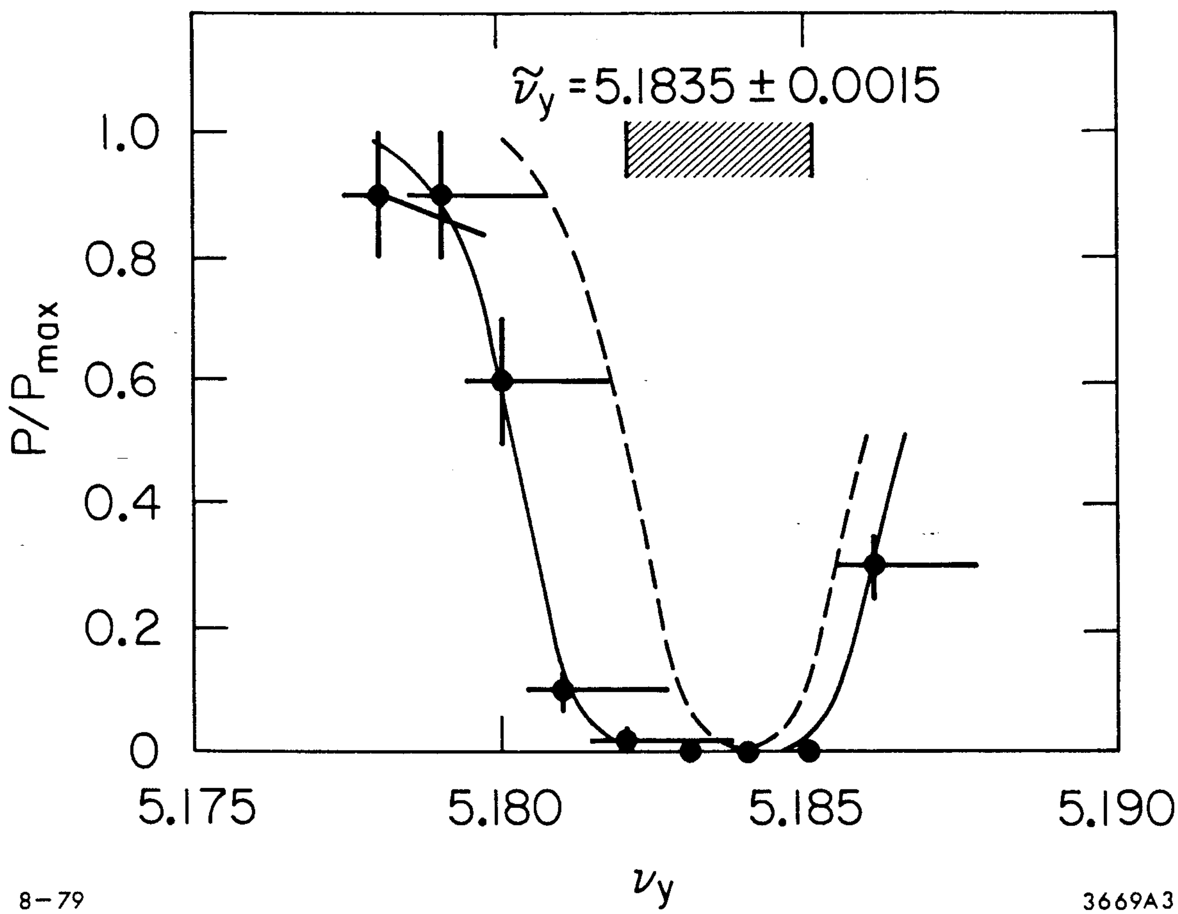
$\tilde{\nu}_y = 5.1835 \pm 0.0015$
1.0
0.8
0.6
0.4
0.2
0
P/P_{max}
5.175
5.180
5.185
5.190
ν_y
8-79
3669A3

Fig. 10

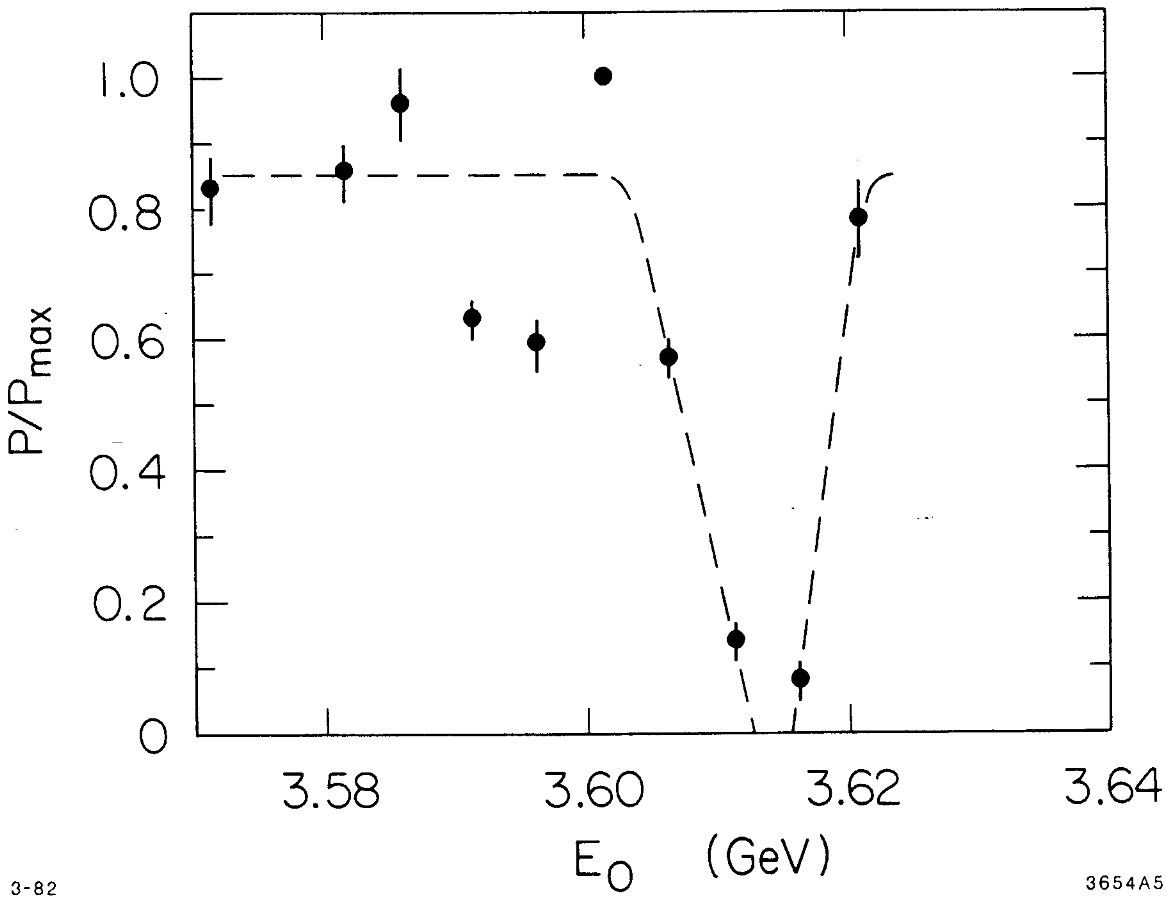

Fig. 11

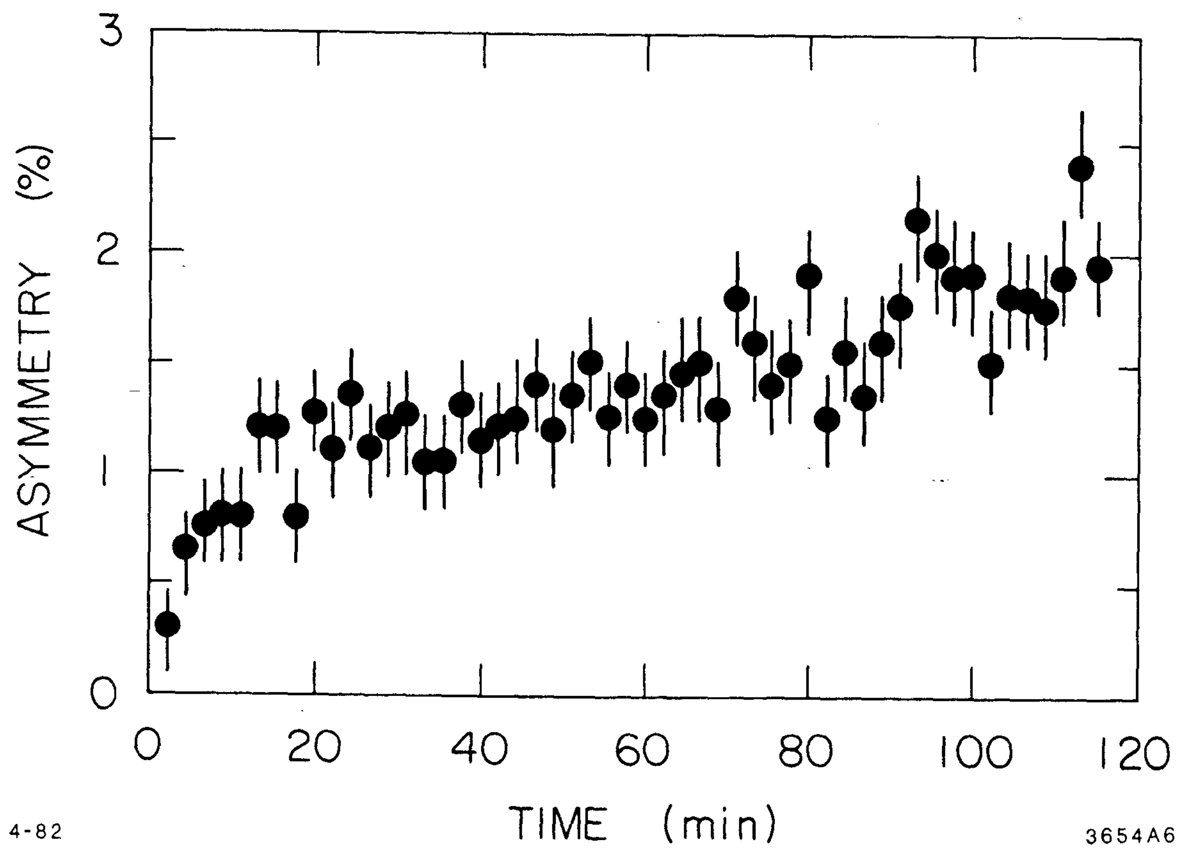

Fig. 12